Materials Research Express

INCLUSIVE PUBLISHING
TRUSTED SCIENCE

PAPER • OPEN ACCESS

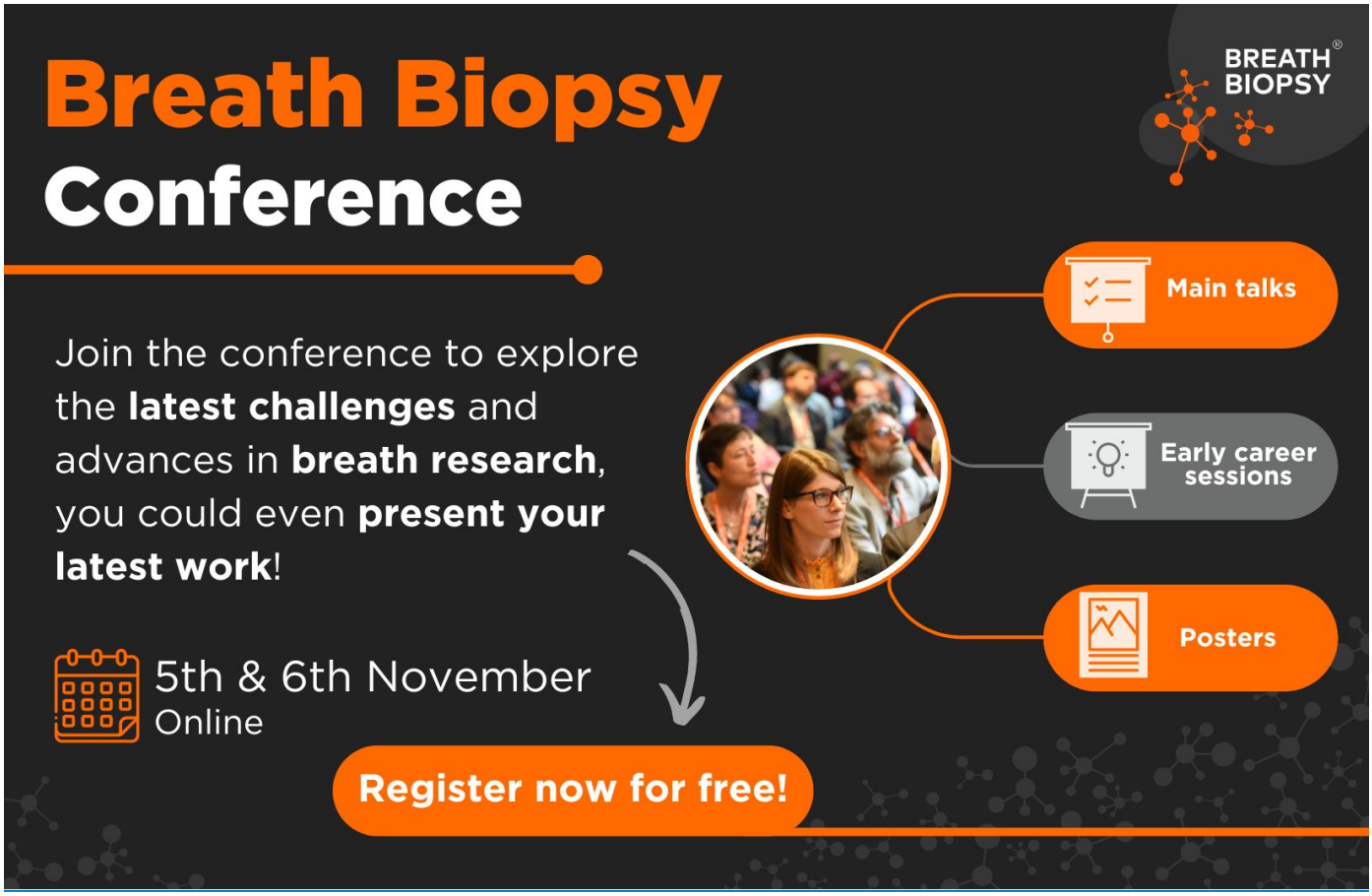
Density functional studies of antimony complexes derived from carboxamide ligands

To cite this article: Berna Çatıkkaş 2023 *Mater. Res. Express* **10** 055402

View the article online for updates and enhancements.

You may also like

- Oral pentamidine-loaded poly(d,l-lactic-co-glycolic) acid nanoparticles: an alternative approach for leishmaniasis treatment
Isabela Viol Valle, Monique Etnea Machado, Cristina da Costa Bernardes Araújo et al.
- Gene expression of some cytokines in patients with Cutaneous leishmaniasis in Al-Diwanyah province
Marwa Hussein Dakeel and Jameel Jerri Yousif
- Recent advances in antifungal drug discovery based on polyene macrolide antibiotics
Olga A. Omelchuk, Anna N. Tevyashova and Andrei E. Shchekotikhin



This content was downloaded from IP address 194.27.44.236 on 25/07/2024 at 16:30

Materials Research Express



OPEN ACCESS

RECEIVED
23 December 2022

REVISED
27 April 2023

ACCEPTED FOR PUBLICATION
4 May 2023

PUBLISHED
15 May 2023

Original content from this work may be used under the terms of the Creative Commons Attribution 4.0 licence.

Any further distribution of this work must maintain attribution to the author(s) and the title of the work, journal citation and DOI.



PAPER

Density functional studies of antimony complexes derived from carboxamide ligands

Berna Çatıkkaş*

Department of Physics, Hatay Mustafa Kemal University, TR-31060 Hatay, Turkey

* Author to whom any correspondence should be addressed.

E-mail: agberna@yahoo.com **and** berna@mku.edu.tr

Keywords: antimony (III) complexes, scale quantum mechanical force field, infrared spectra, DFT, quantum chemical descriptors

Supplementary material for this article is available online

Abstract

The anti-leishmanial activity of antimony (III) complexes [1a-3a] bearing carboxamide ligands has been reported in the literature. In this study, a complete assignment of the vibrational spectra of these complexes was performed using the Scaled Quantum Mechanics Force Field (SQMFF) methodology in the solid phase at the DFT/ B3LYP/ LanL2DZ level. Quantum chemical descriptors (FMO, hardness, softness, etc) of these complexes were calculated to investigate the relationship between the calculated descriptors and their anti-leishmanial activities. As the softness of the complexes increased, the anti-leishmanial activity also increased. No correlation was found between the vibrational frequencies of the complexes and anti-leishmania activity.

1. Introduction

Antimony complexes have various potential uses in the field of health and pharmacy such as anthelminthic [1], antitrypanosomal [2, 3], antimicrobial [4], antifungal [5] and anticancer [6–8] agents. Furthermore, antimony complexes are used popularly as catalysts in organic synthesis [9–11]. Pentavalent antimonials are known to be prodrugs and they are reduced to active Sb (III) form inside the macrophage and parasite cell [12–14].

Antimony (III) complexes have been used for several decades as the first-line treatment for Leishmaniasis, a parasitic disease, caused by protozoa of the genus Leishmania [15], and have contributed significantly to the control and management of this neglected tropical disease [16, 17]. Recently, new antimony (III) chloride complexes [1a–3a] were synthesized (figure 1) and their anti-leishmanial activity was screened [18–22]

While several theoretical calculations have been performed on antimony (III) complexes in previous studies [23–30], few reports on the vibrational analysis of antimony complexes are found in the literature [31]. In this study, we aimed to calculate the vibrational harmonic frequencies of three antimony (III) complexes ([1a–3a]) using the DFT/B3LYP/LanL2DZ level in the Gaussian 09 program. Then the Scaled Quantum Mechanical (SQM) method was used to refine the calculated harmonic frequencies of these complexes in the solid phase. In addition, quantum mechanical descriptors such as hardness, softness, electron affinity, etc of the antimony (III) complexes were calculated to determine whether a relationship between the calculated descriptors and anti-leishmanial activities. Furthermore, the density of state distribution, electronic potential surface map, nonlinear optical properties and hyper-polarizability effects of the antimony (III) complexes were calculated.

2. Computation details

3D structure of the antimony (III) complexes bearing carboxamide ligands used for theoretical calculation was given in figure 1. The quantum chemical calculations were performed using Gaussian 09 software [32] by DFT level using the Lee-Yang-Parr correlation functional (B3LYP) [33–35] methods with LanL2DZ basis set [36–38].

© 2023 The Author(s). Published by IOP Publishing Ltd

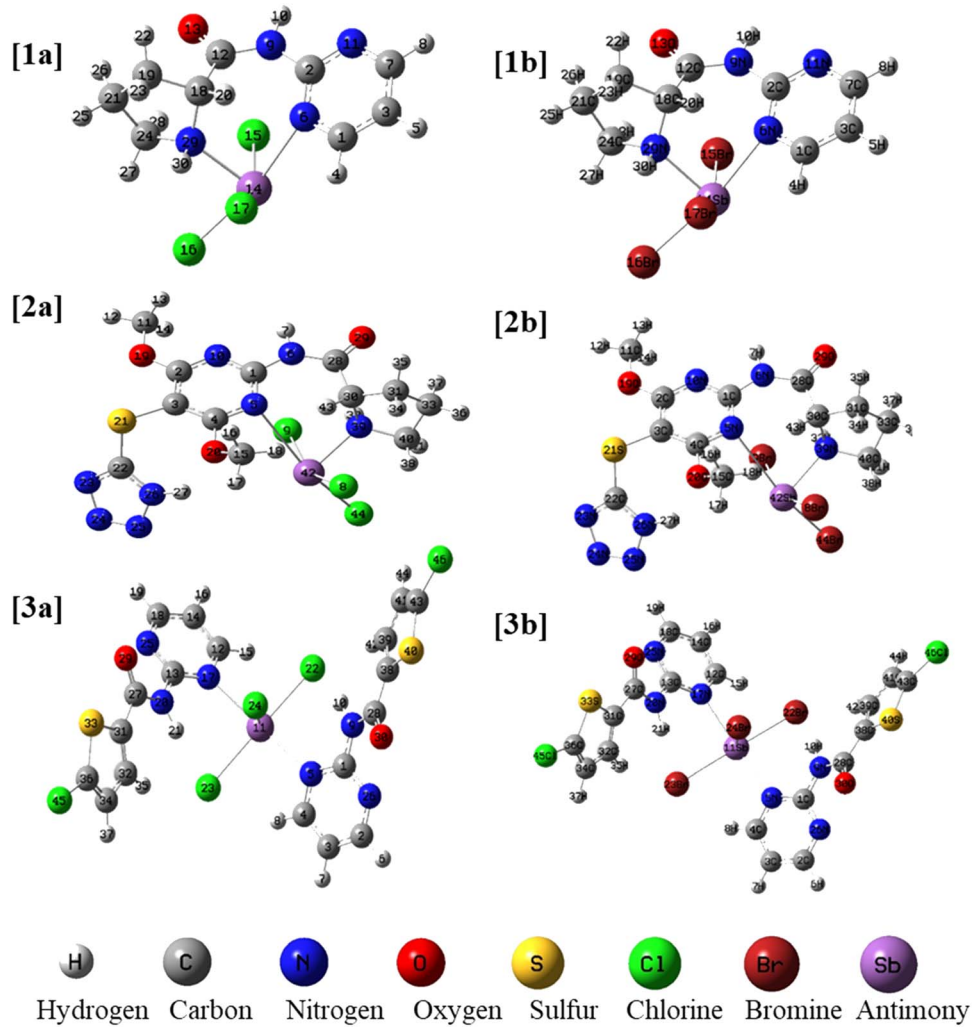


Figure 1. The ground state optimized structure of the complexes.

The dipole moment (μ), the polarizability (α_{tot}) and the first hyperpolarizability (β_{tot}) for the studied compound can be expressed in terms of x, y and z coordinates which are given by the following equations:

$$\mu = (\mu_x{}^2 + \mu_y{}^2 + \mu_z{}^2)^{1/2}$$

$$\alpha_{tot} = 1/3\,(\alpha_{xx} + \alpha_{yy} + \alpha_{zz})$$

$$\beta_{tot} = (\beta_x + \beta_y + \beta_z)^{1/2}$$

where β_i is defined as:

$$\beta_i = (\beta_{iii} + \beta_{ijj} + \beta_{ikk})$$

where, i, j, k = x, y, z.

The Scaled Quantum Mechanical (SQM) Force Field software [39, 40] was used to calculate the scaling DFT force field. Then, the Scaled Quantum Mechanical method was used to refine the calculated frequency in the solid phase.

$$F_{ij}(scaled) = (s_i)^{1/2} F_{ij} (s_j)^{1/2}$$

According to F_{ij}, scaling is applied to the constituents of the internal force constant matrix but not to the particular vibrational wavenumbers. Scaling factors for internal coordinates i and j are si and sj, respectively.

3. Results and discussion

The most stable 3D structures of the antimony (III) complexes with the atom labelling are given in figure 1. Their selected bond lengths and angles are summarized in table S1. The antimony–chloride / bromide bond lengths were consistent with the crystal data [41, 42].

Table 1. Frontier molecular orbital descriptors of the antimony (III) complexes.

Molecular properties (eV)	[1a]	[2a]	[3a]	[1b]	[2b]	[3b]
E_{LUMO}	−2.63	−2.73	−3.11	−2.69	−3.08	−3.21
E_{HOMO}	−7.17	−6.81	−7.54	−6.76	−7.11	−6.82
$\Delta E_{HOMO\text{-}LUMO}$	−4.54	−4.08	−4.42	−4.07	−4.02	−3.61
Ionisation Potential (IP)	7.17	6.81	7.54	6.76	7.11	6.82
Electron Affinity (EA)	2.63	2.73	3.11	2.69	3.08	3.21
Chemical Hardness (η)	**2.27**	**2.04**	**2.21**	**2.03**	**2.01**	**1.80**
Electronegativity (χ)	4.90	4.77	5.33	4.73	5.09	5.01
Chemical Potential (μ)	−4.90	−4.77	−5.33	−4.73	−5.09	−5.01
Softness (S) ev^{-1}	0.44	0.49	0.45	0.49	0.50	0.55
Electrophilicity index (ω)	5.28	5.57	6.41	5.49	6.45	6.96

Table 2. Vibration frequencies with anti-Leishmanialactivity of the antimony (III) complexes.

	[1a]	[2a]	[3a]
νNH	3435	3347	3375
νOC	1702	—	1739
νNC + νCC	1648	1661	1682
νNC + νCC	1606	1620	1634
LC_{50} (M) [22]	8.24×10^{-5}	3.50×10^{-5}	8.39×10^{-5}

3.1. Frontier molecular orbital descriptors

Frontier molecular orbital descriptors of the antimony (III) complexes have been calculated from the energy gap according to Koopmans equations [43, 44], such as chemical potential $\mu = (E_{HOMO} + E_{LUMO})/2$, chemical hardness $\eta = (E_{HOMO}\text{-}E_{LUMO})/2$, global softness $S = 1/\eta$ and electrophilicity index $\omega = \mu^2/2\eta$ to investigate reactivity and stability of the complexes. All descriptors for antimony (III) complexes have been listed in table 1. As seen, there is a correlation between hardness (or softness) and the anti-leishmanial activities of the antimony (III) chloride complexes [1a–3a]. The softest compound [2a] has the highest anti-leishmanial activity. According to the study's findings, bromo antimony (III) complexes, which are predicted to be softer than their chloride antimony (III) counterparts, will have stronger anti-leishmanial activity. [1a] has the second-best anti-Leihmania activity. However, despite efforts to establish a correlation between the vibration frequencies and Anti-Leishmanial activities, no significant correlation was found (table 2).

3.2. The density of state distribution

The density of states is used to determine how many orbitals are available at a given energy level. Partial and Total Density of States (PDOS and TDOS) diagrams were obtained from The Gauss Sum program [45]. The partial density of state plot (PDOS) primarily illustrates the structure of the fragment orbitals that contribute to the molecular orbitals. The calculated PDOS contribution percentage of the antimony (III) complexes was given in table 3. The partial and total density of state distribution PDOS and TDOS spectrum of the complexes are shown in figures 2–4.

As shown in table 3 and figure 2, HOMO is concentrated on N-Sb-X (green line) at a rate of 98 and 99 percent, while LUMO is concentrated on the ring (blue line) at a rate of 69 and 64 percent, [1a] and [1b] respectively. If we look at the molecular orbitals of the [2a] and [2b] complexes they are different from each other (figure 3). In [2a], HOMO is concentrated on other atoms and LUMO is concentrated on 48% N-Sb-Cl. In the [2b], almost all of the HOMO and LUMO are on N-Sb-Br. [3a] and [3b] complexes also have different molecular orbital distribution (figure 4). The HOMO of [3a] is 89% on other atoms (red line) and the LUMO is on 55% N-Sb-Cl (blue line). HOMO and LUMO of [3b] are more on N-Sb-Br.

3.3. NLO effect, dipole moment, polarizability, and hyperpolarizability

To determine nonlinear optical effects, electric dipole moment μ Debye (D), the average polarizability $\Delta\alpha_{tot}$ ($\times 10^{-23}$ esu) and the first hyperpolarizability β_{tot} ($\times 10^{-31}$ esu) of the antimony (III) complexes were calculated with B3LYP/LanL2DZ level, and are listed in table 4. Since the skeleton atoms are usually found on the z-axis, the z value variation tendency for the antimony (III) complexes is similar to the total value. Hyperpolarizability is controlled by the z value and the x and y values also contribute to the hyperpolarizability in a minor way. Among the antimony complexes, [3a] has the highest $\beta_{tot} = 1942.67 \times 10^{-31}$ a.u. and [3b] compound has a relatively

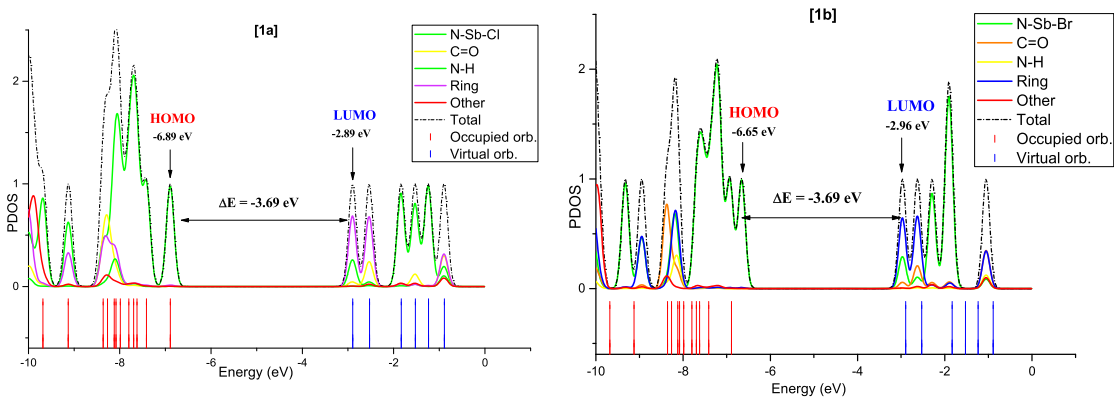


Figure 2. The partial and total density of state distribution PDOS and TDOS spectrum of [1a] and [1b] complexes.

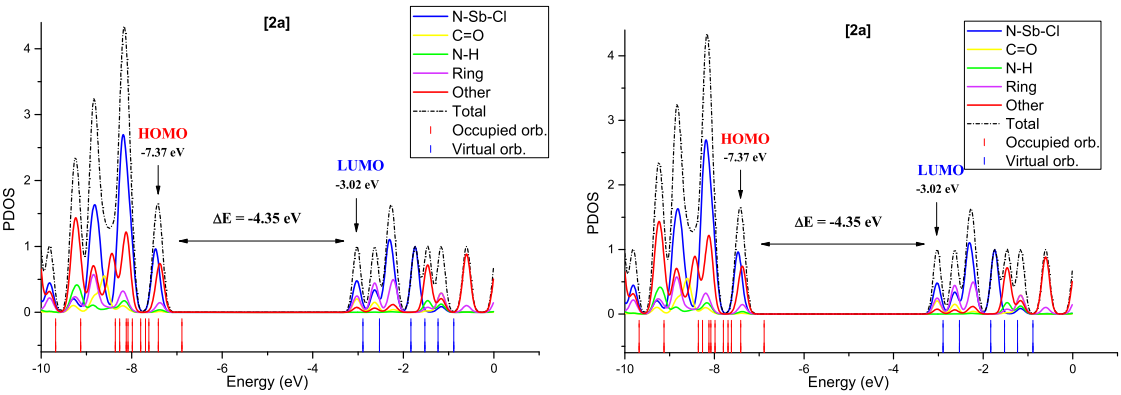


Figure 3. The partial and total density of state distribution PDOS and TDOS spectrum of [2a] and [2b] complexes.

Table 3. The calculated PDOS contribution percentage of the antimony (III) complexes.

		N-Sb-X	N-H	C=O	Ring	Other
[**1a**]	LUMO	26	0	5	69	0
	HOMO	98	0	0	1	0
[**2a**]	LUMO	48	0	20	25	7
	HOMO	10	4	1	14	71
[**3a**]	LUMO	55	1	4	36	3
	HOMO	1	1	7	2	89
[**1b**]	LUMO	29	0	6	64	1
	HOMO	99	0	0	1	0
[**2b**]	LUMO	98	0	0	0	1
	HOMO	99	0	0	0	0
[**3b**]	LUMO	81	1	2	15	1
	HOMO	56	0	3	6	34

higher average polarizability $\Delta\alpha = 787.06$ a.u. value than others. A correlation was observed between the calculated polarizability and electron affinity values of the complexes as well.

3.4. Vibrational spectral analysis

In this study, vibrational harmonic frequencies were calculated by DFT/B3LYP/LanL2DZ level for three antimony complexes [1a–3a]. Assignment of the IR spectra of the antimony (III) complexes has been made based on the calculated potential energy distribution (PED) obtained through the scaled quantum mechanical force field (SQMFF) methodology. RMS values of scaled quantum mechanical (SQM) force field calculation was given in table 5.

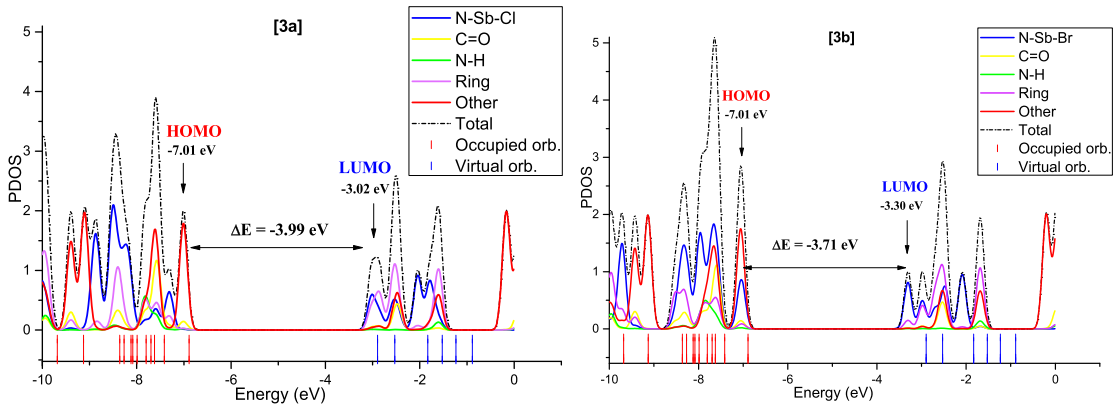


Figure 4. The partial and total density of state distribution PDOS and TDOS spectrum of [3a] and [3b] complexes.

Table 4. Computed electric dipole moment, the average polarizability and hyperpolarizability of the antimony (III) complexes.

μ&α	[1a]	[2a]	[3a]	[1b]	[2b]	[3b]
μ_x	2.71	1.49	0.00	2.85	0.80	0.00
μ_y	0.60	3.50	0.00	−0.68	2.42	3.61
μ_z	1.35	2.46	−3.87	1.07	3.08	0.00
μ (D)	**3.08**	**4.54**	**3.87**	**3.12**	**4.00**	**3.61**
α_{xx}	227.60	336.24	414.80	247.64	400.68	451.21
α_{xy}	−15.81	4.89	70.07	−9.94	38.29	0.03
α_{yy}	188.71	282.85	421.49	235.94	288.05	348.59
α_{xz}	−2.08	21.59	0.03	−19.94	18.43	81.55
α_{yz}	−21.41	−12.21	0.03	−4.71	−18.42	0.03
α_{zz}	154.50	220.16	310.81	173.07	233.35	428.32
$<\alpha>$ (au)	**190.27**	**279.75**	**382.36**	**218.88**	**307.36**	**409.37**
$\Delta\alpha$ (au)	**399.28**	**591.01**	**726.44**	**434.51**	**709.56**	**787.06**
$\Delta\alpha$ ($\times 10^{-23}$ esu)	**5.92**	**8.76**	**10.77**	**6.44**	**10.52**	**11.66**
β_{xxx}	270.04	504.65	2.87	392.96	−225.67	6.10
β_{xxy}	109.69	−311.28	−2.01	26.24	−398.87	226.42
β_{xyy}	161.27	118.87	1.25	9.99	28.78	−5.49
β_{yyy}	−177.30	87.42	2.00	28.29	283.56	554.61
β_{xxz}	66.90	180.95	−447.67	128.10	345.49	1.42
β_{xyz}	2.11	−123.22	−773.24	49.36	−162.25	743.40
β_{yyz}	24.31	21.03	−971.62	−231.58	−185.53	5.57
β_{xzz}	−6.21	−13.00	−2.61	6.28	253.60	−1.22
β_{yzz}	8.24	57.82	−1.61	120.67	138.55	831.38
β_{zzz}	184.94	−38.85	−523.39	170.74	16.07	−1.66
βx	425.10	610.53	1.51	409.23	56.71	−0.61
βy	−59.36	−166.05	−1.63	175.19	23.24	1612.41
βz	276.15	163.13	−1942.67	67.25	176.03	5.33
β_{tot}(a.u.)	**510.39**	**653.39**	**1942.67**	**450.21**	**186.39**	**1612.41**
β_{tot}($\times 10^{-31}$ esu)	44.09	56.45	167.83	38.89	16.10	139.30

α: (1 a.u.) = 0.1482×10^{-24} esu; β; (1 a.u.) = 8.6393×10^{-33} esu

Table 5. RMS values of SQM calculation.

	[1a]	[2a]	[3a]
Pre-fingerprint region	0	2.77	2.91
Fingerprint region (500–2500 cm^{-1})	11.7	5.41	11.38
Post-fingerprint region	4.94	0	2.44
RMS error	10.83	4.86	10.41

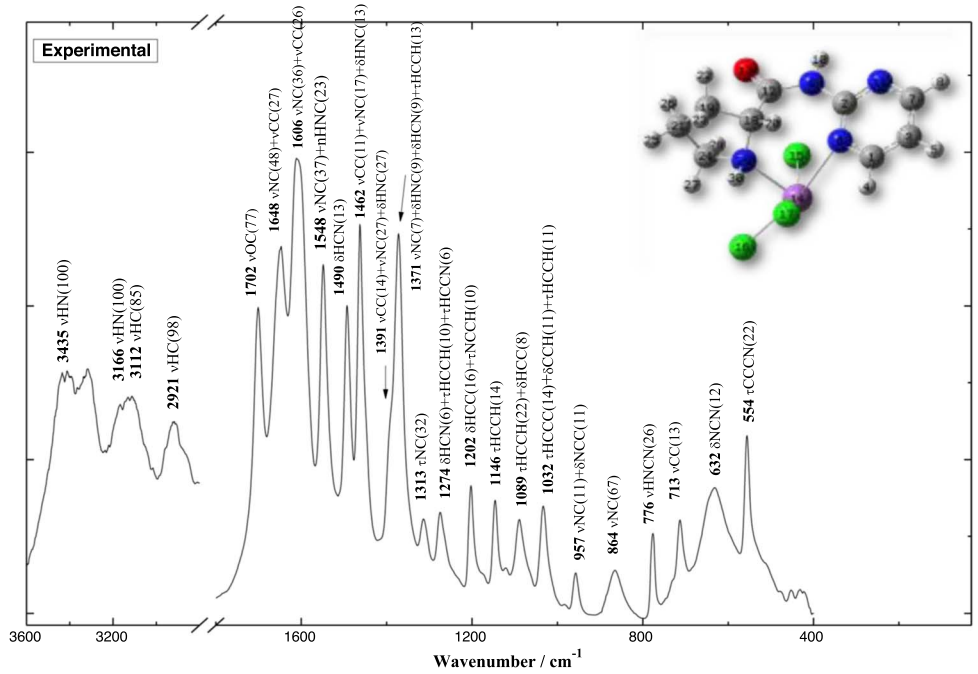


Figure 5. The experimental infrared spectrum of [1a].

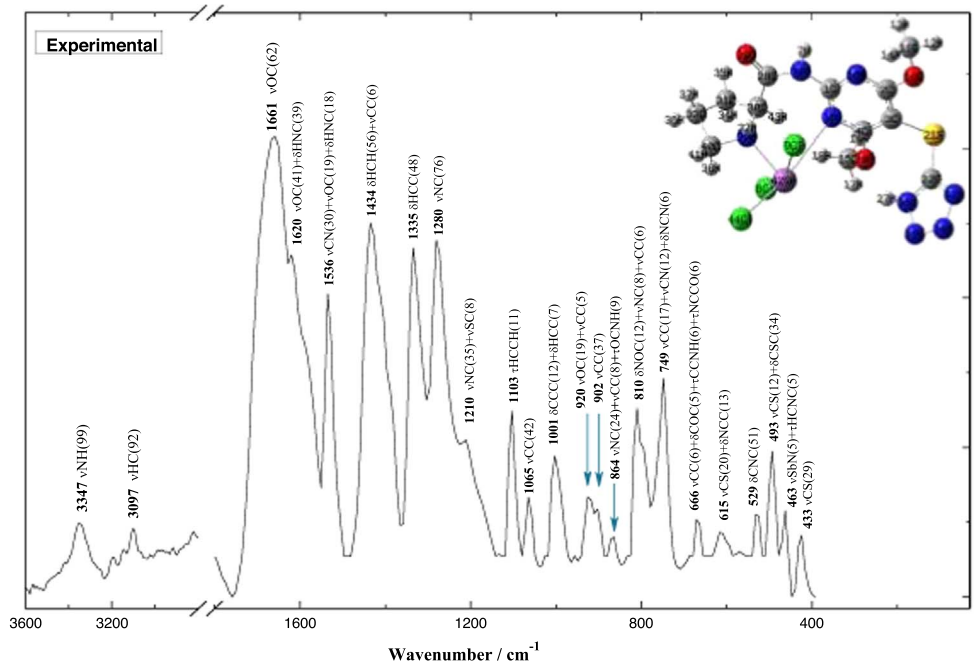


Figure 6. The experimental infrared spectrum of [2a].

Calculated, scaled (SQM) and experimental wavenumbers, intensities and PED are given in tables S2–3. These results showed that the predicted frequencies are well compared with the observed infrared wavenumbers. Experimental infrared spectra of the antimony (III) complexes [1a–3a] with assigned mode are presented in figures 5–7.

3.4.1. C=O vibrations

1702 cm^{-1} [1a] and1739 cm^{-1} [3a] very strong peaks belongs to C=O stretching vibration. In general, a very strong band result from the C=O stretching vibration (1700–1740 cm^{-1}) [46]. The C=O stretching vibration is stronger than the NH stretching vibrations.

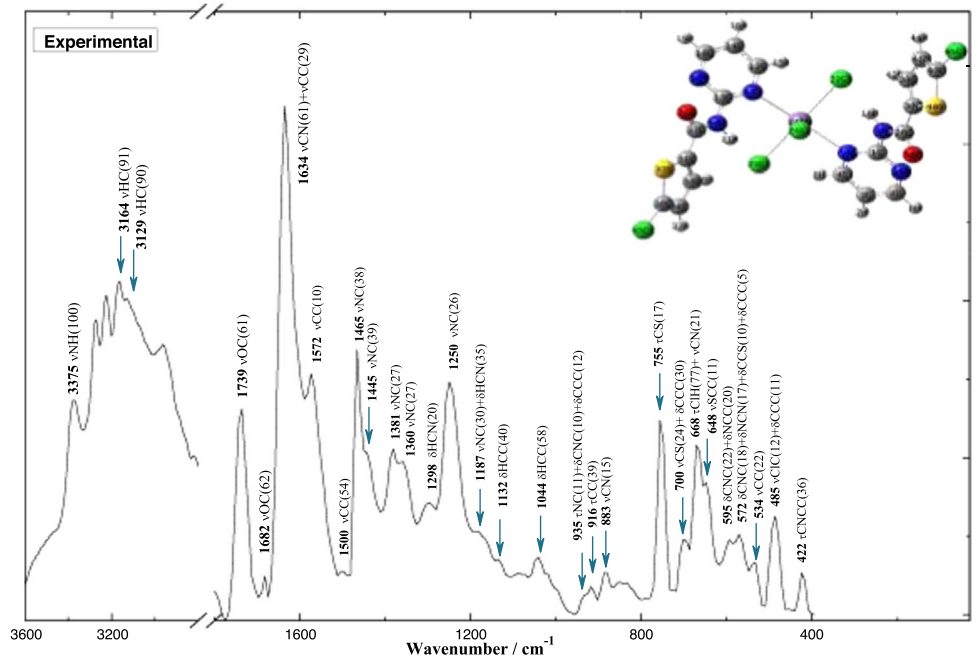


Figure 7. The experimental infrared spectrum of [3a].

3.4.2. NH vibrations

3435 cm^{-1} [1a], 3347 cm^{-1} [2a], and 3375 cm^{-1} [3a] peaks are vibration is a nitrogen and hydrogen stretching vibration (νNH which is located between two different rings).

3.4.3. Aromatic CH and CH_3 group vibrations

It is expected that the typical aromatic C-H stretching vibrations will appear in the wavenumber range of 3000–3200 cm^{-1} [46]. The aromatic C-H stretching vibrations of the [1a] were observed at 3112, 2921 cm^{-1}. Aromatic νC-H of [3a] was calculated at 3160 cm^{-1} in two peaks. 3164 cm^{-1} and C-H bands and 2941 and 2921 cm^{-1} assigned of number [3a] complex. [2a] has CH_3 group: fundamental $\nu(CH_3)$ stretching band appear 3097 cm^{-1}, calculated SQM two peaks are around 3000 cm^{-1}.

3.4.4. C-N vibrations

The calculated peaks 1606, 1648 and 1548 cm^{-1} belong to the CN vibration for [1a]. 1536 cm^{-1} very strong band [2a], and 1634 cm^{-1} very strong band [3a] are CN stretching vibrations observed in the figures 6 and 7 respectively.

3.4.5. S-C, Sb-Cl and Sb-N vibrations

666 cm^{-1} [2a], 755 and 700 cm^{-1} bands [3a] are C-S stretching vibrations [3a]. νSbCl are calculated in the range 228–287 cm^{-1}[1a], 198–232 cm^{-1} [2a], 382–385 cm^{-1} [3a]. δClSbCl are assigned 106–123 cm^{-1} [1a], 98–111 cm^{-1} [2a], 83 cm^{-1} [3a].

4. Conclusion

The harmonic vibrational wavenumbers of three antimony (III) complexes, namely [1a], [2a], and [3a], were calculated using the DFT/B3LYP/LanL2DZ level and subsequently scaled using the Scaled Quantum Mechanics Force Field (SQMFF) method. The scaled quantum mechanical treatment resulted in root mean square deviations of 10.83 cm^{-1} for [1a], 9.69 cm^{-1} for [2a], and 10.41 cm^{-1} for [3a]. The frontier molecular orbital descriptors such as electronegativity, chemical potential, softness, electrophilicity index and electron affinity of the antimony (III) complexes were calculated. It was observed that there is an inverse relationship between the hardness of the complexes and their anti-leishmanial activity. Specifically, as the hardness of the complexes decreases, their anti-leishmanial activity increases. The results of the study led to the prediction that the bromide antimony (III) complexes, which were calculated to be softer than their chloride antimony (III), would exhibit higher anti-leishmanial activity. The results of this study indicate that no correlation exists between the vibration

peaks and anti-leishmanial activities of the antimony (III) complexes. In addition, the calculated polarizability and electron affinity values of the complexes also showed a correlation.

Acknowledgments

This study was supported by the Research Foundation of Hatay Mustafa Kemal University Project No: 16861. I would like to thank Gazi University for providing Gaussian 09 and Scaled Quantum Mechanic Program Software. The numerical calculations reported in this paper were performed at TUBITAK ULAKBIM, High Performance and Grid Computing Center (TRUBA Resources).

Data availability statement

The data cannot be made publicly available upon publication because no suitable repository exists for hosting data in this field of study. The data that support the findings of this study are available upon reasonable request from the authors.

Conflict of interest

No conflict of interest was declared by the authors.

ORCID iDs

Berna Çatıkkaş https://orcid.org/0000-0002-0566-5015

References

[1] Newlove T *et al* 2011 Antihelminthic therapy and antimony in cutaneous leishmaniasis: a randomized, double-blind, placebo-controlled trial in patients co-infected with helminths and leishmania braziliensis *American Journal of Tropical Medicine and Hygiene* **84** 551–54
[2] Navarro M, Gabbiani C, Messori L and Gambino D 2010 Metal-based drugs for malaria, trypanosomiasis and leishmaniasis: recent achievements and perspectives *Drug Discovery Today* **15** 1070–8
[3] Parrilha G L *et al* 2012 2-Acetylpyridine- and 2-benzoylpyridine-derived thiosemicarbazones and their antimony(III) complexes exhibit high anti-trypanosomal activity *Polyhedron* **31** 614–21
[4] Chauhan H P S, Joshi S and Carpenter J 2015 Synthetic, Spectral, Thermal and powder x-ray diffraction studies of bis(O-alkyldithiocarbonato-S,Sâ€2) antimony(III) dialkyldithiocarbamates *Spectrochim. Acta*A **136** 1626
[5] Singhal K, Sahu V K, Singh P and Raj P 2014 DFT-based prediction of antifungal and insecticidal activities of perfluorophenyl antimony(III) and antimony(V) chlorides *Med. Chem. Res.* **23** 1758–67
[6] Ozturk I I *et al* 2013 Synthesis, structural characterization and cytotoxicity of the antimony(III) chloride complex with N,N-dicyclohexyldithiooxamide *Polyhedron* **52** 1403–10
[7] Wang F, Yin H, Yue C, Cheng S and Hong M 2013 Syntheses, structural characterization, in vitro cytotoxicities and DNA-binding properties of triphenylantimony di(N-oxy phthalimide) and di(N-oxy succinimide) complexes *J. Organomet. Chem.* **738** 35–40
[8] Wyllie S and Fairlamb A H 2006 Differential toxicity of antimonial compounds and their effects on glutathione homeostasis in a human leukaemia monocyte cell line *Biochem. Pharmacol.* **71** 257–67
[9] Matsukawa S, Yamamichi H, Yamamoto Y and Ando K 2009 Pentacoordinate organoantimony compounds that isomerize by turnstile rotation *JACS* **131** 3418–9
[10] Dostál L *et al* 2010 [2+ 2] Cycloaddition of carbon disulfide to NCN-chelated organoantimony (III) and organobismuth (III) sulfides: evidence for terminal Sb− S and Bi− S bonds in solution *Organometallics.* **29** 4486–90
[11] Moiseev D V, Morugova V A, Gushchin A V, Shavirin A S, Kursky Y A and Dodonov V A 2004 Tetraphenylantimony carboxylates in the cascade Pd-catalyzed C-phenylation reaction of methyl acrylate in the presence of peroxide *J. Organomet. Chem.* **689** 731–7
[12] Baiocco P, Colotti G, Franceschini S and Ilari A 2009 Molecular basis of antimony treatment in leishmaniasis *J. Med. Chem.* **52** 2603–12
[13] Dos Santos Ferreira C, Silveira Martins P, Demicheli C, Brochu C, Ouellette M and Frézard F 2003 Thiol-induced reduction of antimony(V) into antimony(III): A comparative study with trypanothione, cysteinyl-glycine, cysteine and glutathione *BioMetals.* **16** 441–6
[14] Yan S, Li F, Ding K and Sun H 2003 Reduction of pentavalent antimony by trypanothione and formation of a binary and ternary complex of antimony(III) and trypanothione *J. Biol. Inorg. Chem.* **8** 689–97
[15] Akbari M, Oryan A and Hatam G 2021 Immunotherapy in treatment of leishmaniasis *Immunology Letters.* **233** 80–6
[16] Roatt B M, De Oliveira Cardoso J M, De Brito R C F, Coura-Vital W, De Oliveira Aguiar-Soares R D and Reis A B 2020 Recent advances and new strategies on leishmaniasis treatment *Appl. Microbiol. Biotechnol.* **104** 8965–77
[17] Serban G 2019 Future prospects in the treatment of parasitic diseases: 2-amino-1, 3, 4-thiadiazoles in leishmaniasis *Molecules.* **24** 1557
[18] Tunç T, Koç Y, Açik L, Karacan M S and Karacan N 2015 DNA cleavage, antimicrobial studies and a DFT-based QSAR study of new antimony(III) complexes as glutathione reductase inhibitor *Spectrochim. Acta*A **136** 1418–27
[19] Karacan M S *et al* 2016 Characterization of nineteen antimony(III) complexes as potent inhibitors of photosystem II, carbonic anhydrase, and glutathione reductase *Photosynth. Res.* **130** 167–82
[20] Tunç T, Karacan M S, Ertabaklar H, Sarı M, Karacan N and Büyükgüngör O 2015 Antimony(III) complexes with 2-amino-4,6-dimethoxypyrimidines: Synthesis, characterization and biological evaluation *J. Photochem. Photobiol.*B **153** 206–14

[21] Çiçek İ, Tunç T, Ogutcu H, Abdurrahmanoglu S and Günel A 2020 Synthesis and Antibacterial Activity of New Chiral Aminoalcohol and Benzimidazole Hybrids. *ChemistrySelect* **5** 4650–4
[22] Tunç T, Ertabaklar H and Karacan N 2020 In vitro anti-leishmanial activities and structure-activity relationship analysis of new antimony(III) complexes *Indian J. Chem.*A **59** 1609–17
[23] Schulz A and Villinger A 2012 Binary pnictogen azides-an experimental and theoretical study: $[As(N_3)_4]^-$, $[Sb(N_3)_4]^-$, and $[Bi(N_3)_5(dmso)]^{2-}$ *Chemistry - A European Journal* **18** 2902–11
[24] Fukin G K *et al* 2011 Experimental and theoretical investigation of topological and energetic characteristics of Sb complexes reversibly binding molecular oxygen *J. Phys. Chem.* A **115** 8271–81
[25] Aghabozorg H, Manteghi F, Ghadermazi M, Mirzaei M, Salimi A R and Eshtiagh-Hosseini H 2010 Synthesis, x-ray characterization and molecular structure of a novel supramolecular compound of antimony(III); Theoretical investigation on molecular and electronic properties based on the *ab initio* HF and various DFT methods *J. Iran. Chem. Soc.* **7** 500–9
[26] Wijeratne A B, Gracia J, Yang S H, Kroll P, Armstrong D W and Schug K A 2010 New structural insight for antimony(III)-tartrate *Inorg. Chem. Commun.* **13** 1504–8
[27] Ferreira G B, Hollauer E, Comerlato N M and Wardell J L 2008 An experimental and theoretical study of the electronic spectra of tetraethylammonium [bis(1,3-dithiole-2-thione-4,5-dithiolato)M(III)] and tetraethylammonium [bis(1,3-dithiole-2-one-4,5-dithiolato)M(III)] (M = Sb or Bi) *Spectrochimica Acta - Part A: Molecular and Biomolecular Spectroscopy* **71** 215–29
[28] Poleshchuk O K, Shevchenko E L, Branchadell V, Lein M and Frenking G 2005 Energy analysis of the chemical bond in group IV and V complexes: A density functional theory study *Int. J. Quantum Chem.* **101** 869–77
[29] Jenkins H D B, Krossing I, Passmore J and Raabe I 2004 A computational study of SbnF(5n) (n=1-4) - Implications for the fluoride ion affinity of nSbF(5) *J. Fluorine Chem.* **125** 1585–92
[30] Moc J 2002 Reactions in the SbF5/HF/PF3 system: A DFT and ab initio study *Chem. Phys. Lett.* **363** 328–36
[31] Martins E P S, D O Lima E, Martins F T, De Almeida Vasconcellos M L A and Rocha G B 2019 Synthesis, spectroscopic characterization, DFT studies, and preliminary antimicrobial evaluation of new antimony (III) and bismuth (III) complexes derived from 1, 3, 5-triazine *J. Mol. Struct.* **1183** 373–83
[32] FrischM J *et al* (2016) No Title Gaussian 09, Revision A.02. Gaussian,
[33] Lee C, Yang W and Parr R G 1988 Development of the colle-salvetti correlation-energy formula into a functional of the electron density *Phys. Rev.*B **37** 785–9
[34] Becke A 1993 Density functional thermochemistry III the role of exact exchange *J. Chem. Phys.* **98** 5648–52
[35] Parr R G and Yang W 1989 *Density functional theory of atoms and molecules* (New York: Oxford University Press) 1, 1989
[36] Dunning T H and Hay P J 1977 Gaussian basis sets for molecular calculations BT - methods of electronic structure theory *MApp*. ed H F Schaefer (US, Boston: Springer) 1–27
[37] Hay P J and Wadt W R 1985 Ab initio effective core potentials for molecular calculations. potentials for K to Au including the outermost core orbitals *J. Chem. Phys.* **82** 299–310
[38] Wadt W R and Hay P J 1985 Ab initio effective core potentials for molecular calculations. Potentials for main group elements Na to Bi *J. Chem. Phys.* **82** 284–98
[39] Pulay P, Fogarasi G, Pongor G, Boggs J E and Vargha A 1983 Combination of theoretical ab initio and experimental information to obtain reliable harmonic force constants. Scaled quantum mechanical (QM) force fields for glyoxal, acrolein, butadiene, formaldehyde, and ethylene *JACS* **105** 7037–47
[40] Baker J, Jarzecki A A and Pulay P 1998 Direct scaling of primitive valence force constants: an alternative approach to scaled quantum mechanical force fields *J. Phys. Chem.* A **102** 1412–24
[41] Prokudina Y V *et al* 2020 Structures and chemical bonding in antimony(III) bromide complexes with pyridine *Chemistry—A European Journal* **26** 16338–48
[42] Peng Y-C *et al* 2021 A deep-red-emission antimony (iii) chloride with dual-cations: extremely large Stokes shift due to high [SbCl 6] distortion *Chem. Commun.* **57** 13784–7
[43] Parr R G, Szentpály L V and Liu S 1999 Electrophilicity index *JACS* **121** 1922–4
[44] Koopmans T 1934 Über die zuordnung von wellenfunktionen und eigenwerten zu den einzelnen elektronen eines atoms *Physica* **1** 104–13
[45] O'boyle N M, Tenderholt A L and Langner K M 2008 cclib: a library for package-independent computational chemistry algorithms *J. Comput. Chem.* **29** 839–45
[46] Socrates G 2004 *Infrared and Raman characteristic group frequencies: tables and charts* (England: Wiley)